STUDY ON THE PIECEWISE CONSTANT CURVATURE KINEMATIC MODEL OF A TWO-SEGMENT ROBOT

OLEKSANDR SOKOLOV[1,2], ALEXANDER HOSOVSKY[1], SERHII SOKOLOV[2], BRANISLAV PITEL[1]

[1]Technical University of Kosice, Faculty of Manufacturing Technologies with a seat in Presov, Slovakia

[2]Sumy State University, Ukraine

DOI: 10.17973/MMSJ.2024_12_2024105

oleksandr.sokolov@tuke.sk

ABSTRACT

This study presents the Piecewise Constant Curvature (PCC) kinematic model of a two-segment continuum robot, offering a clear and illustrative approach to deriving the kinematics of a soft manipulator. Analytical expressions are developed to relate the endpoint positions of the robot's pneumatic arm segments to the lengths of its pneumatic muscles. The kinematic model has two contrasting features: it is general enough to be applicable for various continuum robot arms, yet it does not account for specific structural details, requiring adaptation for different soft robot designs. The step-by-step methodology, visual clarity, and extension of the PCC model to a two-segment robot distinguish this research from existing studies. This approach can be extended to multi-segment soft manipulators, offering a valuable framework for further exploration in the field.

KEYWORDS

pneumatic arm, artificial muscle, multi-segment manipulator, transformation matrix

1 INTRODUCTION

Research and innovation have seen significant advancements in soft robotics in recent years, primarily due to enhanced flexibility and safer operations. Researchers have developed new materials, innovative manufacturing technologies, and advanced control methods for soft robots. Consequently, several commercial products, such as soft grippers, are now available on the market and are being utilized in fields such as agriculture, medicine, and engineering [Lin 2019].

Continuum robots, which offer a wide range of applications, are becoming increasingly valuable tools within the robotics community [Webster 2010] as they are more flexible and safer comparing to rigid robots [Tian 2016, Cheng 2020, Lin 2023]. This is mainly because their most valuable characteristics—such as agility in cluttered and unstructured environments and compliant, pliable interactions with objects—differ markedly from those of traditional robots, known for rigidity, precision, and suitability for highly structured environments. Therefore, these robots necessitate corresponding advancements in robotics theory [Webster 2010].

Soft robots are renowned for their ability to facilitate compatible and complex interactions between the robot and its environment. Specifically, soft robotic manipulators or slender robots with a continuum structure can leverage these interactions to provide new possibilities for exploration, manipulation, and safe human-robot interactions. Nevertheless, interactions or disturbances from external forces cause the soft structure to deform in space with an infinite degree of freedom (DOF) [Hosovsky 2016, Stella 2023].

A continuum robot can be defined as a type of robot characterized by an infinite degree of freedom and an elastic structure. However, the ability of these robots to deform with theoretically infinite degrees of freedom presents explicit challenges in modeling and control [Sarosi 2016, Pitel 2014, Tothova 2013 and 2014]. Due to the redundancy in degrees of freedom, continuum robots' perception, planning, and control are still subjects of ongoing research [Cheng 2020].

Furthermore, a continuum robot is typically described as a continuously bending robot with infinite freedom and an elastic structure [Webster 2010]. Continuum robots can assume various shapes due to their unique mechanical design and method of actuation, allowing them to create the desired motion trajectory. This new class of robots exhibits excellent flexibility and agility, thus enabling their application in narrow and unstructured environments [Tian 2016].

It is also important to note that continuum robots are related to hyper-redundant robots, which consist of a finite number of short rigid links but differ in several key aspects. The application of continuum robots in practical scenarios necessitates models that accurately describe the robot's shape and motion. These models must inevitably be more complex than traditional robots, which have a limited number of rigid links [Webster 2010].

One of the primary motivations for developing soft robots is to enhance dynamic movements and compliant interactions. However, rigid robots outperform their soft counterparts in these tasks [Della Santina 2020].

Model-based methods play a crucial role in achieving higher levels of control efficiency in both artificial and natural systems. This observation has led to the development of simplified models capable of describing the robot's behavior using a finite set of variables [Della Santina 2018].

As continuum robots deform, they take on shapes representing general curves in space, making precise control challenging. Due to the practical needs of engineering implementation, the structural design, perception, planning, and control of continuum robots must adhere to certain assumptions, among which the assumption of piecewise constant curvature is widely employed. However, due to the effects of friction and other factors, the motion of an actual continuum robot only approximates piecewise constant curvature [Cheng 2020]. Therefore, the aim of this paper is to propose an approach to describe the kinematics of motion of a continuum robot consisting of 2 segments. In order to achieve this aim, the motion model of the continuum robot has been described, and rotation angles and 3D space coordinates have been determined as a function of the lengths of the pneumatic muscles.

This paper consists of 5 sections. The first section Introduction describes the features of the soft robot and its applications in different fields. The second section describes the approaches that exist in describing the motion of a continuum robot. The third section presents a model that allows describing the kinematics of the motion using a transformation matrix and geometric dependencies. The fourth section discusses the proposed method and the necessity that the development of models account for geometric assumptions, physical phenomena, natural and mechanical processes, material properties, etc. The fifth section Conclusion summarizes the kinematic model of the two-segment robot, showing its adequacy at a qualitative level.

2 LITERATURE REVIEW

One of the fundamental challenges in the field is the accurate description of a continuum robot's shape, commonly achieved through the development of its kinematic model [Lin 2023]. In numerous studies, creating a kinematic model is merely the initial step towards developing other, more complex models. For instance, in [Della Santina 2018], the authors present a dynamic model of soft robots that relies on an underlying kinematic model based on the piecewise constant curvature (PCC) hypothesis. In another study [Wang 2022], a method is proposed for modelling a soft robot that can precisely describe the kinematics during dynamic movements or interactions with the environment. The proposed method facilitates dynamic modelling and control of a multi-segment soft manipulator in three-dimensional space. Additionally, in [Della Santina 2020], two novel algorithms are developed based on a kinematic model, enabling dynamic control of a soft robotic arm and its interaction with the environment.

Over the past decades, many models have been developed, and this process remains active. Researchers frequently modify existing models or propose alternative versions to better suit their specific robotic designs. In most cases, researchers adopt existing models as a foundation and adapt them to their robots' unique features, making necessary modifications.

For example, [Stella 2023] introduces a novel kinematic model based on three-dimensional piecewise affine curvature (PAC). Similarly, [Emet 2024] proposes an alternative method using the PCC approach, expanding the range of models applicable to specific robot designs. However, determining which model most accurately describes a particular robot remains challenging amidst this diversity of models [Gautreau 2022], [Nidhi 2024], [Zhang 2022].

The primary motivation for developing new models is to reduce computational complexity while enhancing the accuracy of kinematic models compared to the classical models based on constant curvature geometry, as described in [Tian 2016]. For instance, [Emet 2024] proposes an alternative method utilizing the PCC approach, which requires less computational overhead yet yields satisfactory results. The authors in [Lin 2023] also argue that calculating direct kinematics is highly complex and computationally intensive, particularly based on geometric considerations. Conversely, [Tian 2016] asserts that a constant curvature kinematic model, grounded in geometric principles, is straightforward to implement and versatile enough to accommodate robots with varying actuation methods.

A step-by-step description demonstrates the mathematical simplicity of using the PCC method to derive a kinematic model for a soft robot. Notably, most kinematic models for soft robots develop simulation and control strategies commonly employed in rigid robots but adapted for soft robotics. For example, [Cheng 2020] proposes a continuous robot kinematics model based on an approximate piecewise constant curvature equivalent to rigid robots' classical kinematics.

Furthermore, [Della Santina 2018] introduces the concept of connecting a soft robot to an equivalent reinforced rigid robot constrained by a set of nonlinear integrable constraints. This approach ensures that the correspondence between the soft robot and its rigid counterpart is accurate within the general constant curvature hypothesis. The authors propose naming the state space of the equivalent rigid robot an extended representation of the states of a soft robot (PCC).

Moreover, [Emet 2024] argues that representing the movement of soft robotic arms within these rigid body modeling environments necessitates a new modeling structure. This requirement arises due to the inadequacy of traditional rigid body modeling approaches. Consequently, this new simulation system must adhere to the same accuracy and computational efficiency standards as traditional solid-state robot models.

According to [Della Santina 2020], such equivalence implicitly determines the relationship between a soft and rigid robot described through equivalent parameterization. From a kinematic perspective, any representation that satisfies the condition of matching the endpoints of each segment of the constant curvature (CC) with the corresponding reference points of the rigid robot is considered equivalent. Therefore, established rigid robot control and analysis knowledge is effectively transferred to soft robots [Wang 2022].

However, unlike the kinematics of traditional rigid-link robots, where the position of any point on the robot can be determined explicitly using link lengths and connection angles, continuum robots' internal compliance necessitates considering elasticity. To accurately determine the positions of points of interest on the robot, including its end-effector, it is essential to account for the forces and moments applied to the robot by its actuators and the external environment [Webster 2010].

Nonetheless, as [Emet 2024] suggests, the established modeling methods and control theories developed for traditional rigid robots are not directly applicable to soft robots. The challenges of kinematic and dynamic modeling of soft robots, which possess infinite degrees of freedom, demand the development of specialized modeling methods.

The piecewise constant curvature (PCC) method is a specialized approach widely employed for simulating the kinematics of continuum robots [Lin 2023]. According to [Wang 2022] and [Della Santina 2018], the PCC method is favored in soft robotics due to its computational efficiency [Emet 2024]. As [Webster 2010] observes, the widespread application of the PCC approach across various continuum robot mechanical architectures, combined with its analytical appeal, underscores its significance in the field.

The PCC method simplifies the modeling of soft robotic arms by representing them as a finite set of mutually tangent arcs of constant curvature, defined by three parameters: the arc length (l), the bending angle (ϑ), and the angle of the plane containing the arc (α). This simplification significantly reduces the number of variables required for the model. Constant curvature is often regarded as a desirable characteristic for continuum robots due to its simplifications for kinematic modeling [Webster 2010].

In the PCC model, the infinite dimensionality of the soft robot's configuration is addressed by considering the robot's shape as comprising a fixed number of segments with CC combined to form a continuously differentiable curve [Della Santina 2020]. It is important to note that the PCC model guarantees the continuity of the form, ensuring that the final frame of one segment and the initial frame of the subsequent segment are seamlessly connected [Lin 2023].

Assuming the PCC model, the continuous robot is composed of constant curvatures, which may change over time, effectively reducing the complexity of the robot's application. However, due to factors such as friction, the actual motion of a continuum robot is often approximated by a piecewise constant curvature (APCC) [Cheng 2020].

In addition to the PCC kinematic model, the parametric modeling method using Denavit-Hartenberg (DH) parameters is gaining popularity for the mathematical description of soft robot motion [Lin 2019], [Webster 2010]. For instance, [Della Santina 2020] employs a kinematic model that can be reformulated using elementary DH transformations to construct a dynamic model.

In conclusion, various modeling approaches converge on a typical outcome for the piecewise constant kinematics of

constant curvature, as reviewed in [Webster 2010]. The ongoing advancements in soft robotics continue to refine these models, enhancing their applicability and accuracy in diverse and challenging environments.

3 RESEARCH METHODOLOGY

This research introduces a methodology for developing a kinematic modeling system, based on an experimental setup depicted in Figure 1. This setup is a modified version of a soft planar robotic arm. The robot manipulator consists of two segments mounted on top of each other. Three artificial muscles control each segment through pressure changes, which also alter the position and orientation of the end-effector. The length of each muscle is 52.4 cm. In each segment, the pneumatic muscles are positioned at an angle of 120° relative to each other. The muscles of the upper and lower segments are offset by an angle of 60°.

The kinematic model of constant curvature was employed based on geometric principles. Upon comparison with the modified Denavit-Hartenberg (DH) method and the finite element method, we determined that this modeling approach is more suitable for continuous robots and offers greater ease of implementation. The kinematic model is based on two fundamental assumptions: (1) the manipulator, when bent, can be approximated as an arc of a circle, and (2) gravitational effects are neglected in the kinematic modeling process.

The position and orientation of the manipulator can be controlled by altering the length of the rods, and the constant curvature method, based on geometric principles, is employed to develop the kinematic model of the continuum robot. A mapping between the configuration space, manipulation space, and task space is obtained to facilitate the analysis of the kinematics.

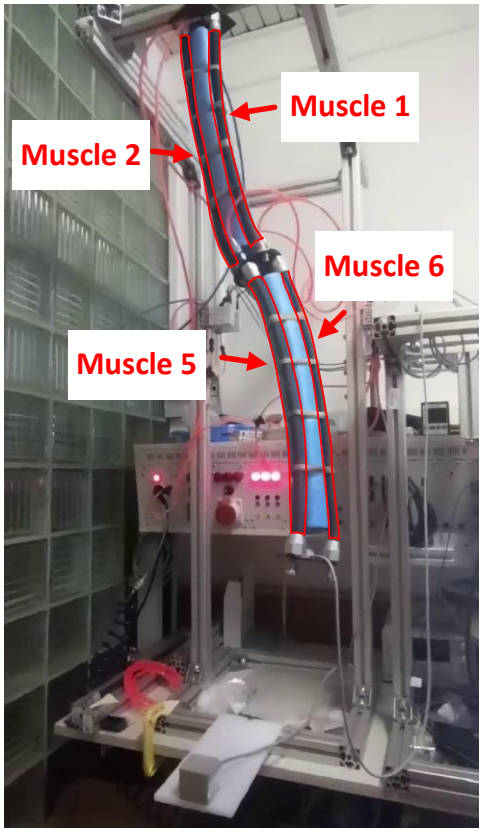

Figure 1. Experimental Setup

Selecting coordinate axes

Consider a kinematic model of a soft robot composed of two segments with piecewise constant curvature (PCC) (Figure 2).

In the literature, there is a broad range of conventions, formalisms, and variants of coordinate systems for achieving direct kinematics [Tian 2016]. Some of these approaches will be utilized in this research.

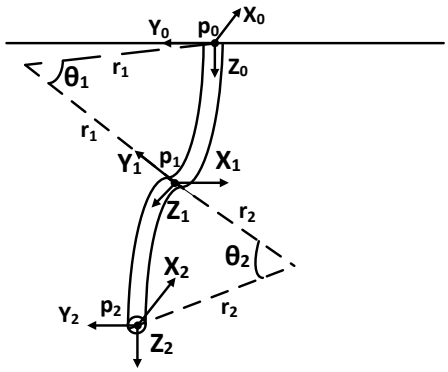

Figure 2. Kinematic model of the robot

The axes are chosen as follows. The origin of the coordinate system is located at the center of the base of the first segment, with the z_0 axis aligned along the muscle and serving as the reference for the coordinate system. This point is denoted as p_0. The x_0 and y_0 axes can be chosen arbitrarily, provided they are mutually perpendicular and perpendicular to the z_0 axis. The y_0 axis is oriented in the direction of the muscle's bending, with the bending angle denoted by ϑ.

The position of the x_0 axis is determined by the right-hand rule with respect to the y_0 and z_0 axes. The angle of rotation of the muscle around the z_0 axis is denoted by α. When $\alpha = 0$, the direction of muscle bending by the angle ϑ lies within the y_0–z_0 plane. The rotation of the muscle around the z_0 axis by an angle α is described in the x_0–y_0 plane.

The matrix of motion can be written in the following form:

$$\mathbf{T} = \begin{bmatrix} \mathbf{R} & \mathbf{p} \\ 0 & 1 \end{bmatrix}, \tag{1}$$

where **R** represents the rotation matrix; **p** is the translation vector.

Determining the coordinate of the end of the first segment

Consider the planar case where there is only bending of the segment without rotation, i.e. the angle $\alpha = 0$. When α is zero, the arc lies entirely within the *y-z* plane, as depicted in Figure 3. In this scenario, the bending is described solely by the angle ϑ, which defines the curvature of the segment within the plane. The absence of rotation ($\alpha = 0$) simplifies the transformation, restricting the motion to the *y-z* plane.

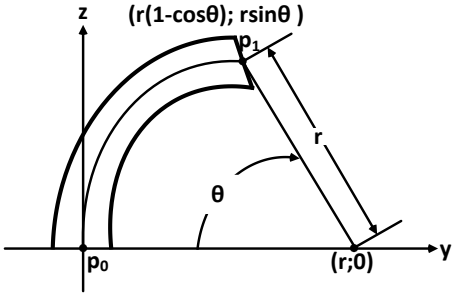

Figure 3. Geometric representation of the arc of the pneumatic muscle in the *y-z* plane at $\alpha = 0$

The bending is considered to occur along an arc with a radius r and an angle ϑ. The coordinates of the lower point p_0 and the upper point p_1 of the cylinder in the spherical coordinate system are determined accordingly. As illustrated in Figure 3, the lower point p_0 of the manipulator in the *y-z* plane is represented by the coordinates $p(r,0)$, where r denotes the radius of the arc. To determine the coordinates of the upper point p_1, geometric construction, as shown in Figure 4, is employed.

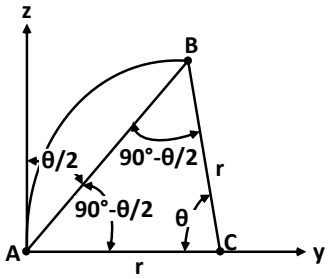

Figure 4. Determining the arc rotation angle ϑ

The resulting triangle ABC is isosceles with the base AB, as *AC = BC = r*. Therefore, the angles ∠*A* and ∠*B* are equal and can be calculated by using formula (2)

$$(180° - \theta)/2 = 90° - \theta/2 . \quad (2)$$

The projection of point B (the endpoint of the segment) onto the *y*-axis can be expressed as follows. From Figure 5, it can be observed that y_1 is equal to the subtraction between *r* and *DC*. On the other hand, *DC* is given by $r \cdot \cos\theta$ Therefore, it can be written as the equation:

$$y_1 = r - r \cdot \cos\theta = r(1-\cos\theta). \quad (3)$$

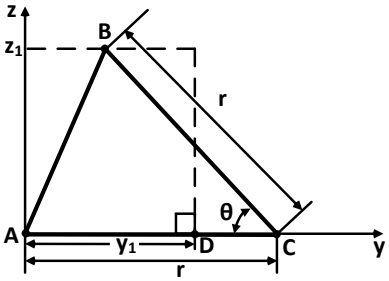

Figure 5. Determination of the coordinates of the endpoint p_1 of the arc at $\alpha = 0$

The projection of the B on the *z*-axis can be written by the following expression:

$$z_1 = BD = r \cdot \sin\theta . \quad (4)$$

Therefore, in two-dimensional space, the coordinates of the top point will be as follows:

$$p_1(r \cdot (1-\cos\theta);\ r \cdot \sin\theta). \quad (5)$$

Considering the rotation of the segment around the *z*-axis within the *x*-y plane by an angle *α* (as illustrated in Figure 6), the projection of the endpoint onto the *x*-axis can be expressed as, $r \cdot \cos\alpha$, while the projection onto the y-axis can be expressed as $r \cdot \sin\alpha$.

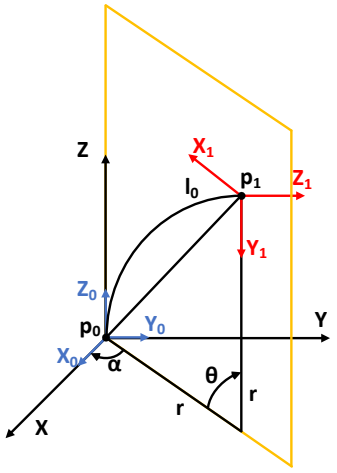

Figure 6. Determination of coordinates of point p_1 of the arc at $\alpha \neq 0$

Accordingly, the coordinates of the endpoint of the segment can be represented as:

$$p_{1x} = r \cdot (1-\cos\theta) \cdot \cos\alpha , \quad (6)$$

$$p_{1y} = r \cdot (1-\cos\theta) \cdot \sin\alpha , \quad (7)$$

$$p_{1z} = r \cdot \sin\alpha . \quad (8)$$

The position of the end point in the 3-dimensional coordinate system will have the coordinates:

$$p_1\ (r \cdot (1-\cos\theta) \cdot \cos\alpha;\ r \cdot (1-\cos\theta) \cdot \sin\alpha;\ r \cdot \sin\theta) . \quad (9)$$

Determining the rotation matrix

At this stage, it is essential to determine the rotation matrices around the *z* and *y* axes. The rotation matrix around the *z*-axis, denoted as $\boldsymbol{R_z}$, is commonly referred to as the rotation matrix. This matrix describes the transformation from the initial coordinates x_0,y_0 to the new coordinates x_1,y_1, while the *z*-coordinate remains unchanged. Consequently, the rotation of the *x* and *y* axes occurs by an angle *α* within the *x*-*y* plane, as depicted in Figure 7.

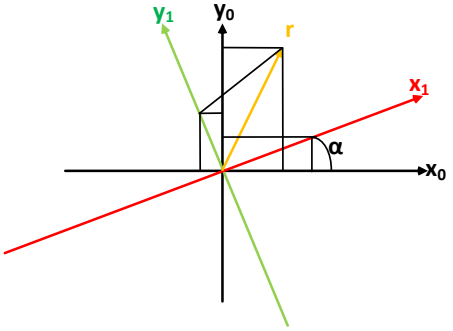

Figure 7. Determination of coordinates of point p_1 of the arc at $\alpha \neq 0$

The dependence between the x_0,y_0 and the x_1,y_1 coordinates can be written as a system of equations:

$$\begin{cases} x_1 = a_{11} \cdot x_0 + a_{12} \cdot y_0 + a_{13} \cdot z_0 \\ y_1 = a_{21} \cdot x_0 + a_{22} \cdot y_0 + a_{23} \cdot z_0 \\ z_1 = a_{31} \cdot x_0 + a_{32} \cdot y_0 + a_{33} \cdot z_0 \end{cases} \quad (10)$$

Figure 7 shows that $a_{11} = a_{22} = \cos\alpha$, $a_{12} = -\sin\alpha$, $a_{21} = \sin\alpha$. Since the projection of the *z*-axis onto *x* and *y* is a point, the coefficients $a_{13} = a_{23} = 0$ and $a_{33} = 1$, since the z_0 and z_1 axes are directed perpendicular to the plane of the figure and are completely coincident. As a result, we can write the following rotation matrix:

$$\mathbf{R}_z = \begin{bmatrix} \cos\alpha & -\sin\alpha & 0 \\ \sin\alpha & \cos\alpha & 0 \\ 0 & 0 & 1 \end{bmatrix}. \quad (11)$$

Similarly, the rotation matrix around the *y*-axis, denoted as $\mathbf{R_y}$, is constructed. In this case, the same reasoning applied to the $\mathbf{R_z}$ matrix is used, with the substitution of *z* for *y*. As a result, the following matrix can be obtained as:

$$\mathbf{R}_y = \begin{bmatrix} \cos\theta & 0 & \sin\theta \\ 0 & 1 & 0 \\ -\sin\theta & 0 & \cos\theta \end{bmatrix}. \quad (12)$$

The rotation matrix **R** can be determined by multiplying matrices $\mathbf{R_z}$ and $\mathbf{R_y}$ as follows:

$$\mathbf{R}=\mathbf{R}_z\times\mathbf{R}_y=\begin{bmatrix}\cos\alpha & -\sin\alpha & 0\\ \sin\alpha & \cos\alpha & 0\\ 0 & 0 & 1\end{bmatrix}\cdot\begin{bmatrix}\cos\theta & 0 & \sin\theta\\ 0 & 1 & 0\\ -\sin\theta & 0 & \cos\theta\end{bmatrix}=$$

$$=\begin{bmatrix}\cos\alpha\cdot\cos\theta & -\sin\alpha & \cos\alpha\cdot\sin\theta\\ \sin\alpha\cdot\cos\theta & \cos\alpha & \sin\alpha\cdot\sin\theta\\ -\sin\theta & 0 & \cos\theta\end{bmatrix}. \quad (13)$$

The transformation matrices for rotational **R** and translational **P** movements are combined. The resulting kinematic homogeneous transformation relationship can be expressed as follows:

$$\mathbf{T}=\begin{bmatrix}\cos\alpha\cdot\cos\theta & -\sin\alpha & \cos\alpha\cdot\sin\theta & r\cdot\cos\alpha\cdot(1-\cos\theta)\\ \sin\alpha\cdot\cos\theta & \cos\alpha & \sin\alpha\cdot\sin\theta & r\cdot\sin\alpha\cdot(1-\cos\theta)\\ -\sin\theta & 0 & \cos\theta & r\cdot\sin\theta\\ 0 & 0 & 0 & 1\end{bmatrix}. \quad (14)$$

It is important to note that the resulting transformation matrix is robot-independent, as it is applicable to all systems that can be approximated as piecewise-continuous arcs of constant curvature. This reasoning is supported by the works of other authors who describe kinematic models of soft robots [Gautreau 2022], [Nidhi 2024].

Determining the rotation matrix and coordinates of the end of the second segment

Since the robot consists of two segments connected in series, this connection can be described by multiplying the transformation matrices that represent these segments. Let the coordinates *r*, θ, and *α* of the first and second segments be denoted by the indices 1 and 2, respectively. Additionally, it is important to account for the specific design feature of the robot, which involves a horizontal plane shift by an angle of 60° at the points where the two segments are connected. Thus, the kinematics of the robot can be determined by two homogeneous transformations $\mathbf{T_1}$ and $\mathbf{T_2}$, which map each reference frame to the subsequent one. Based on the above considerations, the transformation matrices for each of the segments can be expressed as follows:

$$\mathbf{T}_1=\begin{bmatrix}\cos\alpha_1\cdot\cos\theta_1 & -\sin\alpha_1 & \cos\alpha_1\cdot\sin\theta_1 & r_1\cdot\cos\alpha_1\cdot(1-\cos\theta_1)\\ \sin\alpha_1\cdot\cos\theta_1 & \cos\alpha_1 & \sin\alpha_1\cdot\sin\theta_1 & r_1\cdot\sin\alpha_1\cdot(1-\cos\theta_1)\\ -\sin\theta_1 & 0 & \cos\theta_1 & r_1\cdot\sin\theta_1\\ 0 & 0 & 0 & 1\end{bmatrix}, \quad (15)$$

$$\mathbf{T}_2=\begin{bmatrix}\cos(\alpha_2+\frac{\pi}{3})\cdot\cos\theta_2 & -\sin(\alpha_2+\frac{\pi}{3}) & \cos(\alpha_2+\frac{\pi}{3})\cdot\sin\theta_2 & r_2\cdot(\alpha_2+\frac{\pi}{3})\cdot(1-\cos\theta_2)\\ \sin(\alpha_2+\frac{\pi}{3})\cdot\cos\theta_2 & \cos(\alpha_2+\frac{\pi}{3}) & \sin(\alpha_2+\frac{\pi}{3})\cdot\sin\theta_2 & r_2\cdot\sin(\alpha_2+\frac{\pi}{3})\cdot(1-\cos\theta_2)\\ -\sin\theta_2 & 0 & \cos\theta_2 & r_2\cdot\sin\theta_2\\ 0 & 0 & 0 & 1\end{bmatrix}. \quad (16)$$

After multiplying the transformation matrices and performing the transposition operation, the expressions for the endpoint of the second segment $\mathbf{p_2}$ can be determined as follows:

$$p_{2x}=a_{14}=r_2\cdot\left(\cos\alpha_1\cdot\cos(\alpha_2+\frac{\pi}{3})\cdot\cos\theta_1\cdot(1-\cos\theta_2)\right)-$$

$$-r_2\cdot\left(\sin\alpha_1\cdot\sin\left(\alpha_2+\frac{\pi}{3}\right)\cdot(1-\cos\theta_2)+\cos\alpha_1\cdot\sin\theta_1\cdot\sin\theta_2\right) \quad (17)$$

$$p_{2y}=a_{24}=r_2\cdot\left(\sin\alpha_1\cdot\cos(\alpha_2+\frac{\pi}{3})\cdot\cos\theta_1\cdot(1-\cos\theta_2)\right)+$$

$$+r_2\cdot\left(\cos\alpha_1\cdot\sin\left(\alpha_2+\frac{\pi}{3}\right)\cdot(1-\cos\theta_2)\right)+ \quad (18)$$

$$+r_2\cdot(\sin\alpha_1\cdot\sin\theta_1\cdot\sin\theta_2)+r_1\cdot\sin\alpha_1\cdot(1-\cos\theta_1),$$

$$p_{2z}=a_{34}=r_2\cdot\left(-\cos\left(\alpha_2+\frac{\pi}{3}\right)\cdot\sin\theta_1\cdot(1-\cos\theta_2)+\cos\theta_1\cdot\cos\theta_2\right)+$$

$$+r_1\cdot\sin\theta_1. \quad (19)$$

Therefore, to determine the final position of the robot arm, it is necessary to know six parameters: the radii r_1 and r_2, and the angles α_1, α_2, θ_1 and θ_2. These parameters can be expressed in terms of the muscle lengths l_1, l_2, l_3, l_4, l_5, l_6.

Determining of segment coordinates by muscle lengths

The relationships between the model parameters and the dimensions of the robot will first be established for a single segment. The center of the manipulator and each of the muscles will have different radii of curvature. The relationship between them can be expressed based on Figure 8 and Figure 9.

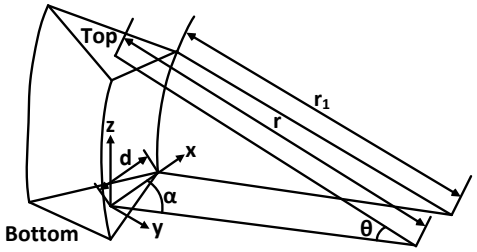

Figure 8. Determination of radius and angles (side view)

Here, *r* represents the radius of curvature of the manipulator, r_1 denotes the radius of curvature of the muscle, and *d* is the distance from the center of the base plane to the center of the flexible rod (as shown in Figure 8). The variable α_i describes the angle between the direction of the manipulator's curvature and the position of the *i*-th rod. From Figure 8, it can be observed that:

$$r_i=r-d\cdot\cos\alpha_i. \quad (20)$$

The relationship between the radius *r*, the angle θ, and the arc length *l* is given by the following equation:

$$l_i=r_i\cdot\theta. \quad (21)$$

Thus,

$$r_i=\frac{l_i}{\theta} \quad (22)$$

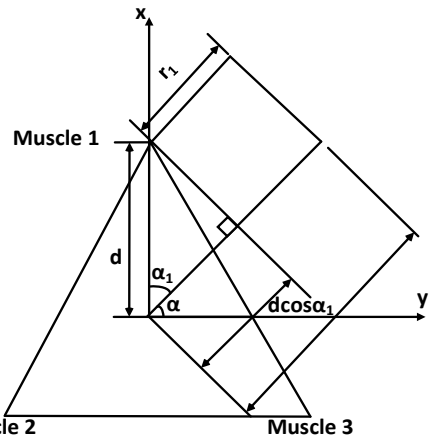

Figure 9. Determination of radius and angles (top view)

For the pair of muscles 1 and 2, the subtraction between the radii can be expressed as:

$$r_1-r_2=\frac{l_1-l_2}{\theta}=d\cdot(\cos\alpha_1-\cos\alpha_2)\cdot \quad (23)$$

From this relationship, it can be derived that:

$$\theta \cdot d = \frac{l_1 - l_2}{\cos\alpha_1 - \cos\alpha_2}. \quad (24)$$

Similarly, for the pair of muscles 1 and 3, the relationship can be expressed as follows:

$$\theta \cdot d = \frac{l_1 - l_3}{\cos\alpha_1 - \cos\alpha_3}. \quad (25)$$

Equating expressions (24) and (25) yields:

$$\frac{l_1 - l_2}{\cos\alpha_1 - \cos\alpha_2} = \frac{l_1 - l_3}{\cos\alpha_1 - \cos\alpha_3}. \quad (26)$$

Since the muscles are positioned at an angle of 120° relative to each other, it can be assumed that $\alpha_1 = \alpha$, $\alpha_2 = \alpha + \frac{2\pi}{3}$, $\alpha_2 = \alpha - \frac{2\pi}{3}$. Therefore, expression (26) can be rewritten as follows:

$$(l_1 - l_2)\cdot\left(\cos\alpha - \cos\left(\alpha - \frac{2\pi}{3}\right)\right) =$$
$$= (l_1 - l_3)\cdot\left(\cos\alpha - \cos\left(\alpha + \frac{2\pi}{3}\right)\right). \quad (27)$$

According to trigonometric identities:

$$\cos\left(\alpha \pm \frac{2\pi}{3}\right) = -\frac{1}{2}\cdot\cos\alpha \mp \frac{\sqrt{3}}{2}\cdot\sin\alpha. \quad (28)$$

Therefore, the expression can be reformulated as follows:

$$(l_1 - l_2)\cdot\left(\cos\alpha - \left(-\frac{1}{2}\cdot\cos\alpha + \frac{\sqrt{3}}{2}\cdot\sin\alpha\right)\right) =$$
$$= (l_1 - l_3)\cdot\left(\cos\alpha - \left(-\frac{1}{2}\cdot\cos\alpha - \frac{\sqrt{3}}{2}\cdot\sin\alpha\right)\right), \quad (29)$$

$$\left[(l_1 - l_3) - (l_1 - l_2)\right]\cdot\frac{3}{2}\cos\alpha = \left[(l_1 - l_3) + (l_1 - l_2)\right]\cdot\frac{\sqrt{3}}{2}\sin\alpha. \quad (30)$$

Therefore, the tangent of the angle α can be expressed in terms of the muscle lengths as follows:

$$\tan\alpha = \frac{\sin\alpha}{\cos\alpha} = \frac{3\cdot(l_2 - l_3)}{\sqrt{3}\cdot(l_2 + l_3 - 2\cdot l_1)}. \quad (31)$$

Utilizing the trigonometric identity $1 + \tan^2\alpha = \frac{1}{\cos^2\alpha}$ and equation (31), the expressions for the cosine and sine of the angle α can be written as functions of the muscle lengths as follows:

$$\cos\alpha = \frac{1}{\sqrt{1 + \tan^2\alpha}} = \frac{l_2 + l_3 - 2\cdot l_1}{2\cdot\sqrt{l_1^2 + l_2^2 + l_3^2 - l_1\cdot l_2 - l_2\cdot l_3 - l_1\cdot l_3}}, \quad (32)$$

$$\sin\alpha = \tan\alpha\cdot\cos\alpha = \frac{\sqrt{3}\cdot(l_2 - l_3)}{2\cdot\sqrt{l_1^2 + l_2^2 + l_3^2 - l_1\cdot l_2 - l_2\cdot l_3 - l_1\cdot l_3}}. \quad (33)$$

From expression (31), it follows that:

$$\alpha = \tan^{-1}\left(\frac{3\cdot(l_2 - l_3)}{\sqrt{3}\cdot(l_2 + l_3 - 2\cdot l_1)}\right). \quad (34)$$

Therefore, the rotation angle α of the muscle in the horizontal plane can be expressed as a function of the lengths l_i of each muscle in the segment. To express the radius of curvature r in terms of the muscle lengths, it is important to consider that:

$$\theta = \frac{l_i}{r_i} = \frac{l}{r}. \quad (35)$$

By substituting equation (20) into equation (35), the following expression can be obtained:

$$r_i = \frac{l_i\cdot r}{l} = r - d\cdot\cos\alpha_i, \quad (36)$$

$$r = \frac{l - l_i}{l} = d\cdot\cos\alpha_i. \quad (37)$$

From expression (37), the formula for the radius of curvature can be derived as follows:

$$r = \frac{l\cdot d\cdot\cos\alpha_i}{l - l_i}. \quad (38)$$

Since the muscles have equal lengths in the initial position, the length of the centerline l of the robot arm can be determined as the average value of the sum of the lengths of each muscle:

$$l = \frac{l_1 + l_2 + l_3}{3}. \quad (39)$$

To calculate the radius r of the robot arm, the first muscle is selected, where $\alpha_i = \alpha$ and $l_i = l_1$. Substituting equations (32) and (39) into equation (38) yields:

$$r = \frac{l\cdot d\cdot\cos\alpha}{l - l_1} = \frac{(l_1 + l_2 + l_3)}{(l_1 + l_2 + l_3 - 3\cdot l_1)}\cdot d\cdot\frac{l_2 + l_3 - 2\cdot l_1}{2\cdot\sqrt{l_1^2 + l_2^2 + l_3^2 - l_1\cdot l_2 - l_2\cdot l_3 - l_1\cdot l_3}} =$$
$$= \frac{l_1 + l_2 + l_3}{2\cdot\sqrt{l_1^2 + l_2^2 + l_3^2 - l_1\cdot l_2 - l_2\cdot l_3 - l_1\cdot l_3}}. \quad (40)$$

Therefore, the radius of curvature r of the arm has been expressed in terms of the lengths l_i of each muscle within this segment. The angle θ can be determined by substituting equations (39) and (40) into equation (35).

$$\theta = \frac{1}{r} = \frac{(l_1 + l_2 + l_3)}{3}\cdot\frac{2\cdot\sqrt{l_1^2 + l_2^2 + l_3^2 - l_1\cdot l_2 - l_2\cdot l_3 - l_1\cdot l_3}}{(l_1 + l_2 + l_3)\cdot d} =$$
$$= \frac{2}{3d}\cdot\sqrt{l_1^2 + l_2^2 + l_3^2 - l_1\cdot l_2 - l_2\cdot l_3 - l_1\cdot l_3}. \quad (41)$$

A similar approach can be applied to the second segment by substituting the muscle lengths l_1, l_2 and l_3 with l_4, l_5 and l_6. To determine the position of the robot arm's endpoint along the *X*, *Y*, and *Z* axes, it is sufficient to substitute the obtained values of the angle α (from equation 34), the radius r (from equation 40), and the angle θ (from equation 41), which are dependent on the muscle lengths, into expressions (17) – (19).

4 DISCUSSION

Continuum robots are indisputably a significant and actively explored domain within the scientific community. This is substantiated by the extensive body of literature concerning their modeling, experimental investigations, the application of contemporary data processing technologies, and review articles that seek to identify common methodologies, phenomena, and patterns.

One of the primary objectives in the operation of continuum robots is the precise control of their movement, which necessitates establishing a clear correlation between the control inputs and the coordinates of the end effector of the pneumatic arm. To determine such a relationship, a kinematic model is sufficient. In our case, the end of the pneumatic arm can be manipulated by varying the length of each pneumatic muscle, achieved by altering the air pressure within them

[Mizakova 2014]. Thus, our research is focused on deriving the kinematic model of the continuum robot. We posit that the approach to modeling should be grounded in theories that are universally applicable to any structure, such as those found in mathematics, geometry, and trigonometry. We firmly believe that all formulas must be either visually or analytically substantiated through mathematical operations. This does not preclude the use of software and computational tools for data acquisition and processing. Our research has aimed to describe the kinematic model of a soft robot (Figure 1), based on the PCC (Piecewise Constant Curvature) model, mathematical operations, and the properties of trigonometric functions. Despite the complexity of the PCC model and the significant computational resources it demands, as noted by authors [Emet 2024], [Lin 2023], [Wang 2022], we present a clear method for obtaining the kinematic model of a soft manipulator composed of two segments. Moreover, we do not concur with the assertion that the computation of trigonometric functions and multiplications entails "significant computational costs" given the current state of computational technology. The comprehensive sequence of operations, the ability to verify each step, and the extension of the PCC model to a two-segment robot are the distinguishing features of our research compared to existing studies. Naturally, we recognize that the development of models must account for geometric assumptions (e.g., deviations in robot curvature from a constant), physical phenomena (such as friction and hysteresis effects), changes in properties depending on environmental parameters (e.g., variations in size and elasticity), natural processes (e.g., aging, microcrack formation, changes in elasticity), mechanical processes, material properties, and the technical implementation of robots.

5 CONCLUSION

In this study, we have presented the kinematic analysis of a pneumatic arm of a generalized continuum robot, consisting of two segments. The proposed approach, however, is extendable to multi-segment soft manipulators. The kinematic model developed exhibits two distinct characteristics: it is, on one hand, sufficiently general to be applicable to various continuum robot arms, yet, on the other hand, it only partially incorporates specific structural features. Furthermore, the model does not account for physical phenomena such as thermal expansion and hysteresis, typically addressed by dynamic models. A comprehensive understanding of a robot's behavior necessitates the integration of the kinematic model, which defines the robot's shape, with both static and dynamic models.

The kinematic model can demonstrate adequacy when evaluated qualitatively; however, its quantitative accuracy warrants experimental validation. The iterative process of experiment-model-experiment-model, and so on, facilitates the development of generalized models through experimental data obtained from specific continuum robot structures. This procedure will be the subject of our further research in this area. Then these models can be applied to the study and design of robots with different configurations. So, in our subsequent research, we will compare the simulation results with experimental data obtained from a soft planar robotic arm (Figure 1) and a methodology for model adaptation will be proposed. This methodology will offer a significant potential for advancing the study of the kinematics of various types of soft robots.

ACKNOWLEDGMENTS

This research was funded by the EU NextGenerationEU through the Recovery and Resilience Plan for Slovakia under the projects No. 09I03-03-V03-00075, No. 09I03-03-V01-00095. This work was also supported by the projects VEGA 1/0061/23, KEGA 022TUKE-4/2023 granted by the Ministry of Education, Research, Development and Youth of the Slovak Republic.

REFERENCES

[Cheng 2020] Cheng, H., Liu, H., Wang, X., Liang, B. Approximate piecewise constant curvature equivalent model and their application to continuum robot configuration estimation. In: 2020 IEEE Int. Conf. on Systems, Man, and Cybernetics (SMC), IEEE, 2020, pp. 1929-1936.

[Della Santina 2018] Della Santina, C., Katzschmann, R.K., Biechi, A., Rus, D. (2018). Dynamic control of soft robots interacting with the environment. In: 2018 IEEE Int. Conf. on Soft Robotics (RoboSoft), IEEE, 2020, pp. 46-53.

[Della Santina 2020] Della Santina, C., Katzschmann, R.K., Bicchi, A., Rus, D. Model-based dynamic feedback control of a planar soft robot: Trajectory tracking and interaction with the environment. The International Journal of Robotics Research, 2020, Vol. 39, No. 4, pp. 490-513.

[Emet 2024] Emet, H., Gur, B., Dede, M.I.C. The design and kinematic representation of a soft robot in a simulation environment. Robotica, 2024, Vol. 42, No. 1, pp. 139-152.

[Gautreau 2022] Gautreau, E., et al. Kinematic modelling of a bioinspired two sections serial continuum robot (SCR). In: A. Muller, M. Brandstötter (Eds.), Advances in service and industrial robotics. RAAD 2022. Mechanisms and machine science, 2022, Vol. 120. Springer, Cham, pp. 247-255.

[Hosovsky 2016] Hosovsky, A. et al. Dynamic characterization and simulation of two-link soft robot arm with pneumatic muscles. Mechanism and Machine Theory, 2016, Vol. 103, pp. 98-116.

[Lin 2019] Lin, P.T., Shahabi, E., Yang, K.A., Yao, Y.T., Kuo, C.H. Parametrically modeled DH table for soft robot kinematics: Case study for a soft gripper. In: T. Uhl (Ed.), Advances in mechanism and machine science. IFToMM WC 2019. Mechanisms and machine science, 2019, Vol. 73. Springer, Cham, pp. 617-625.

[Lin 2023] Lin, S., Wang, Y., Li, A., Chen, W. The piecewise constant curvature model for the forward and inverse kinematics of continuum robot based on Lie theory. In: 2023 Int. Conf. on Advanced Robotics and Mechatronics (ICARM), IEEE, 2023, pp. 386-391.

[Mizakova 2014] Mizakova, J., Pitel, J., Tothova, M. Pneumatic Artificial Muscle as Actuator in Mechatronic System. Applied Mechanics and Materials, 2014, Vol. 460, pp. 81-90.

[Nidhi 2024] Nidhi, S.N., Sooraj, V. Bio-inspired skeletal model and kinematics of humanoid spine and ribs. Proceedings of the Institution of Mechanical Engineers, Part C: J. of Mechanical Engineering Science, 2024, Vol. 238, No. 1, pp. 94-107.

[Pitel 2013] Pitel, J., Tothova, M. Dynamic Modelling of PAM Based Actuator Using Modified Hill´s Muscle Model. In: Proceedings of the 2013 14th International Carpathian Control Conference (ICCC), Rytro, 26-29, May, 2013. Danwers: IEEE, 2013, pp. 307-310.

[Sarosi 2017] Sarosi, J., et al. Comparative Survey of Various Static and Dynamic Models of Pneumatic Artificial Muscles. Transactions of the Canadian Society for Mechanical Engineering, 2017, Vol. 41, No. 5, pp. 825-844.

[Stella 2023] Stella, F., Guan, Q., Leng, J., Della Santina, C., Hughes, J. Piecewise Affine Curvature model: A reduced-order model for soft robot-environment interaction beyond PCC. In: 2023 IEEE Int. Conf. on Soft Robotics (RoboSoft), 2023, pp. 1-7.

[Tian 2016] Tian, Y., Luan, M., Gao, X., Wang, W. and Li, L. Kinematic analysis of continuum robot consisted of driven flexible rods. Mathematical Problems in Engineering, 2016. https://doi.org/10.1155/2016/6984194

[Tothova 2013] Tothova, M., Pitel, J. Dynamic Model of Pneumatic Actuator Based on Advanced Geometric In: IEEE 9th Int. Conf. on Computational Cybernetics (ICCC), Tihany, 8-10, July, 2013. Danwers: IEEE, 2013, pp. 83-87.

[Tothova 2014] Tothova, M., Pitel, J., Mizakova, J. Electro-pneumatic robot actuator with artificial muscles and state feedback. Applied Mechanics and Materials, 2014, Vol. 460, pp. 23-31.

[Wang 2022] Wang, Z., Wang, G., Chen, X., Freris, N.M. Dynamical modeling and control of soft robots with non-constant curvature deformation. 2022. DOI: 10.48550/arXiv.2203.07929.

[Webster 2010] Webster, R.J., Jones, B.A. Design and kinematic modeling of constant curvature continuum robots: A review. The International Journal of Robotics Research, 2010, Vol. 29, No. 13, pp. 1661-1683.

[Zhang 2022] Zhang, G., et al. Design and modeling of a bio-inspired compound continuum robot for minimally invasive surgery. Machines, 2022, Vol. 10, No. 6, 468.

CONTACTS:

Mgr. Oleksandr Sokolov
Assoc. Prof. Ing. Alexander Hosovsky, PhD.
Assoc. Prof. Serhii Sokolov, PhD.
Ing. Branislav Pitel

Technical University of Kosice

Faculty of Manufacturing Technologies with a seat in Presov

Department of Industrial Engineering and Informatics

Bayerova 1, 080 01 Presov, Slovakia

+421 950 235 775

oleksandr.sokolov@tuke.sk; alexander.hosovsky@tuke.sk; s.sokolov@ksu.sumdu.edu.ua; branislav.pitel@tuke.sk